



## An effective and selective stable metal-organic framework adsorbent (Al-MOF-5) for the removal of fluoride from water

Xingang Wang<sup>a</sup>, Kai Liu<sup>a</sup>, Hui Zhu<sup>a</sup>, Tongshuai Sun<sup>a</sup>, Ting Han<sup>a</sup>, Jialiang Li<sup>b,\*</sup>, Hongliang Dai<sup>a,c,d,\*</sup>

<sup>a</sup>School of Environmental and Chemical Engineering, Jiangsu University of Science and Technology, No. 2 Mengxi Road, Zhenjiang 212018, China, Tel. +86-0511-8563-5850; emails: daihongliang103@163.com/daihongliang@just.edu.cn (H. Dai), hofs@just.edu.cn (X. Wang), 1980662745@qq.com (K. Liu), 18252588451@163.com (H. Zhu), 18252588460@163.com (T. Sun), hanting970424@163.com (T. Han)

<sup>b</sup>School of Chemistry and Chemical Engineering, Shandong University of Technology, Zibo 255000, China, email: lijialiang@sdut.edu.cn

<sup>c</sup>Jindalai Environmental Protection Co., Ltd., Jiangxi 330100, China

<sup>d</sup>School of Environmental and Engineering, Huazhong University of Science and Technology, Wuhan 430074, China

Received 19 May 2020; Accepted 19 November 2020

### ABSTRACT

A novel aluminum (Al)-containing Al-MOF-5 metal-organic framework (MOF) material for the removal of fluoride from the water was prepared using a hydrothermal method. The structure of the resulting product was characterized by scanning electron microscopy, transmission electron microscopy, X-ray diffraction, thermogravimetry, Brunauer, Emmett, and Teller nitrogen adsorption, Fourier transform-infrared spectroscopy, and X-ray photoelectron spectroscopy methods. In batch tests, the effects of adsorbent dosage, pH, and temperature were studied. Result showed that the maximum adsorption capacity of adsorbent for fluoride was 46.08 mg/g. The Langmuir isotherm model and pseudo-second-order kinetics fitted the adsorption process well and the thermodynamics indicated that the adsorption of fluoride on the material was spontaneously endothermic. The Al-MOF-5 displayed a high removal rate of more than 70% at different pHs, and the only  $\text{PO}_4^{3-}$  could affect its adsorption efficiency for fluoride. Finally, Al-MOF-5 that had been regenerated six times in NaOH solution at a concentration of 0.3 mol/L still achieved a removal rate of nearly 50% for 10 mg/L fluoride solution.

**Keywords:** Adsorption; Fluoride removal; Metal-organic framework (Al-MOF-5)

### 1. Introduction

About 70% of the Earth's surface is covered by water, but 97% of this is highly saline seawater. Furthermore, more than 2% of the water is concentrated at the north and south poles, and less than 1% of the water is available for human use [1]. Most of the freshwater used by humans is obtained from rivers, lakes, and groundwater. The chemical characteristics of such waters largely determine whether

or not they can be fully exploited by humans. Excessive fluoride ( $\text{F}^-$ ) in natural waters is predominantly caused by the discharge of fluoride-rich wastewater effluent, or by surface water washing of fluoride-containing ore over long periods [2–4]. High fluoride concentrations are very harmful, and poor water quality is an important problem facing human societies. To protect human health, the World Health Organization (WHO) stipulates a maximum safe concentration of fluoride in drinking water of 1.5 mg/L;

\* Corresponding authors.

in China, the concentration is 1.0 mg/L [5]. There are more than 200 million people worldwide who drink water with excessive fluoride content. Research from Rasool et al. [6] showed that high-fluoride water is widely distributed in the World. Long-term consumption of high-fluoride water can lead to fluorosis, which is a chronic systemic disease. When excessive fluoride enters the human body, it is deposited mainly on teeth and bones, leading to dental and skeletal fluorosis, which seriously affect bone health and liver and kidney function in young children [7–9].

Extensive research aimed at reducing the fluoride content of high-fluoride water has been conducted. Fluoride removal from drinking water has primarily been attempted using coagulation, ion exchange, membrane separation, reverse osmosis, and adsorption methods [10–14]. Adsorption methods to remove fluoride from water, which involves the use of an adsorbent, ion exchange, or complexation, are the most well-researched and widely used because of their simplicity, stability, and low cost. Many different materials are used as defluorination adsorbents, including metal oxides, natural mineral adsorbents, and activated carbon [15]. The good adsorption performance of activated alumina is due to its large specific surface area, dense pore structure, and ability to form chemical bonds with F<sup>-</sup>. Activated alumina is recognized by the WHO and the United States Environmental Protection Agency (US EPA) as the best fluoride-removing adsorbent [16]. Although activated alumina is positively charged, its adsorption capacity is only 0.5–2.0 mg/g. Furthermore, it quickly reaches saturation and has poor regeneration ability. Although modification of activated alumina has been extensively studied, increasing its adsorption capacity remains a challenge [17].

As a possible solution to these issues, the metal-organic frameworks (MOFs), which are crystalline porous materials having a periodic network structure composed of a porous metal center (metal ions or metal clusters) and bridging organic ligands, gradually attracted people's attention. MOFs have enormous specific surface areas and have been widely studied in catalysis, gas separation, gas storage, and many other fields; however, the application of MOFs to water treatment remains largely unexplored [18–20].

In recent years, great attention has been devoted to the application of MOF-5 materials in chemistry. MOF-5 (also known as IRMOF-1) was prepared by reacting zinc ions (Zn<sup>2+</sup>) with 1,4-benzenedicarboxylic acid (H<sub>2</sub>BDC) in *N,N*-dimethylformamide (DMF) solution under specific conditions [21]. This MOF has a relatively stable crystal structure and well-developed methods are available for its synthesis. Aluminum (Al) is an abundant and inexpensive element that binds more strongly with fluoride than many other adsorbents. It is also an excellent adsorbent for other low-concentration contaminants [22]. The adsorption mechanisms include physical adsorption, chemical adsorption, and ion exchange. In an Al-containing defluorination adsorbent, Al<sup>3+</sup> ions provide abundant active sites and high charge, which improves the adsorption capacity of fluoride [23,24].

In our study, we replaced the Zn<sup>2+</sup> metal center in MOF-5 with Al<sup>3+</sup> to form the new Al-MOF-5, and investigated its ability to remove fluoride from drinking water. The new Al-MOF-5 combines the large specific surface area of MOF-5 with the rich active centers of Al<sup>3+</sup>, which

improves the adsorption capacity of fluorine. The effects of adsorbent dosage, initial concentration, pH, and coexisting anions on the adsorption properties of Al-MOF-5 were studied in detail. Isothermal, kinetic, and thermodynamic analyses were performed to investigate the adsorption behavior of this material. Finally, the material was regenerated to study its performance after regeneration. The material was characterized using numerous analytical techniques, to determine the adsorption mechanism of this adsorbent for defluorination.

## 2. Experiment section

### 2.1. Materials

Aluminum nitrate nonahydrate (Al(NO<sub>3</sub>)<sub>3</sub>·9H<sub>2</sub>O), 1,4-benzenedicarboxylate (H<sub>2</sub>BDC), *N,N*-dimethylformamide (DMF), and sodium hydroxide were provided by Sinopharm Chemical Reagent Co., Ltd., (Shanghai, China). Sodium fluoride was provided by Tianjin Kaitong Chemical Reagent Co., Ltd., (Tianjin, China). Alizarin complexone (fluoride reagent, molecular formula: C<sub>19</sub>H<sub>15</sub>NO<sub>8</sub>) was provided by Tianjin Komiou Chemical Reagent Co., Ltd., (Tianjin, China). Distilled water was used throughout the experiment, all chemicals, and reagents were of analytical grade and used as received without further purification.

### 2.2. Fabrication of Al-MOF-5

Al-MOF-5 was synthesized by a solvothermal method. In detail, aluminum nitrate nonahydrate (Al(NO<sub>3</sub>)<sub>3</sub>·9H<sub>2</sub>O, 99.99%, 1.0365 g) and 1,4-benzenedicarboxylic acid (H<sub>2</sub>BDC, 99.00%, 0.178 g) were dissolved in DMF (99.90%, 20 mL), and then stirred ultrasonically until the solids had completely dissolved. The solution was then transferred to a 50 mL reaction tube with a Teflon liner for solvothermal treatment at 393 K for 4 h. After cooling to room temperature, the obtained white precipitate was separated by centrifugation and washed three times with DMF. The precipitate was then washed with distilled water, and the white powder thus obtained was vacuum-dried at 333 K overnight.

### 2.3. Characterization

S-4800 field emission scanning electron microscopy (Hitachi, Japan), Tecnai 12 instrument X-ray diffraction (XRD, Philips, Netherlands) and D8 advance diffractometer (Bruker, Germany) were used to obtain the scanning electron microscopy (SEM) images, the transmission electron microscopy (TEM) images, and XRD spectrometry patterns, respectively. The Brunauer, Emmett, and Teller (BET) data and thermogravimetric (TG) data of Al-MOF-5 were measured by an ASAP 2460 automatic surface area and porosity analyzer (Micromeritics, USA) and Pyris Diamond TG-TGA (PerkinElmer, USA2). The characterization of the nascent as well as the spent Al-MOF-5 were done using an ESCALAB 250Xi spectrometer (Thermo Fisher, USA) and a Nicolet NEXUS 470 Fourier transforms infrared (FTIR) spectroscopy (Thermo Fisher, USA) to get X-ray photoelectron spectrometer (XPS) experiments data and FTIR data,

while the absorbance value of fluoride in aqueous solution was determined by a UV755B UV-visible spectrophotometer (Aoyi, China).

#### 2.4. Fluoride adsorption experiment

The effects of initial fluoride concentration, adsorbent dosage, contact time, initial pH, and coexisting anions on the adsorption performance of Al-MOF-5 was studied. Experiments were conducted in 250 mL plastic Erlenmeyer flasks. The initial fluoride solutions were dilutions of a fluoride standard stock solution having a fluoride concentration of 1 g/L. The adsorption procedure was as follows. A prescribed amount of adsorbent was added to the flask containing the fluoride solution, which was then placed in a constant-temperature shaker at 200 rpm for fixed times. The concentration of fluoride in the solution was determined by fluoride reagent spectrophotometry. The solution was filtered through a 0.22  $\mu\text{m}$  cellulose membrane before measuring the absorbance of the solution using an ultraviolet-visible spectrophotometer at a wavelength of 620 nm. Then, the fluoride concentration in the solution was calculated using the fluoride standard curve (linear equation:  $y = 0.302x + 0.0067$ , where  $x$  is the concentration of fluoride and  $y$  is the absorbance value (goodness of fit,  $R^2 = 0.9996$ ). The adsorption capacity ( $q_e$ , mg/g) and removal percentage ( $R$ , %) were calculated as follows (Eqs. (1) and (2)):

$$q_e = \left( \frac{C_0 - C_e}{m} \right) V \quad (1)$$

$$R = \left( \frac{C_0 - C_e}{C_0} \right) \times 100\% \quad (2)$$

where  $C_0$  and  $C_e$  (mg/L) are the initial and final fluoride concentration,  $V$  (L) is the volume of the solution, and  $m$  is the weight of the Al-MOF-5, respectively.

Solutions of NaOH and HNO<sub>3</sub> (each 1 mol/L) were used to adjust the initial pH of the solution, and NaCl, Na<sub>2</sub>SO<sub>4</sub>, NaNO<sub>3</sub>, Na<sub>2</sub>CO<sub>3</sub>, and Na<sub>3</sub>PO<sub>4</sub> were used to add coexisting anions to the solution. The effect of pH on fluoride adsorption was examined by using the NaOH and HNO<sub>3</sub> solutions to adjust the pH of 100 mL of fluoride solution having a fluoride concentration of 10 mg/L. In this way, the pH ranged from 3 to 11 and the coexisting anion concentration in the solution ranged from 0 to 20 mg/L. The solution having an anion concentration of 0 mg/L was used as the blank. Adsorption experiments were carried out for 12 h at room temperature; the adsorbent was then removed by filtration and the fluoride concentration in the filtrate was determined.

To reduce the cost, we prepared Al-MOF-5 using the solvent method, isolated the used Al-MOF-5 by centrifugation, and regenerated it by reheating. The post-regeneration performance was assessed by repeated treatment of the regenerated Al-MOF-5 with the different solutions.

### 3. Results and discussion

#### 3.1. Characterization of Al-MOF-5

SEM and TEM revealed the Al-MOF-5 morphology. The SEM image at 100.0 K magnification (Fig. 1a) shows

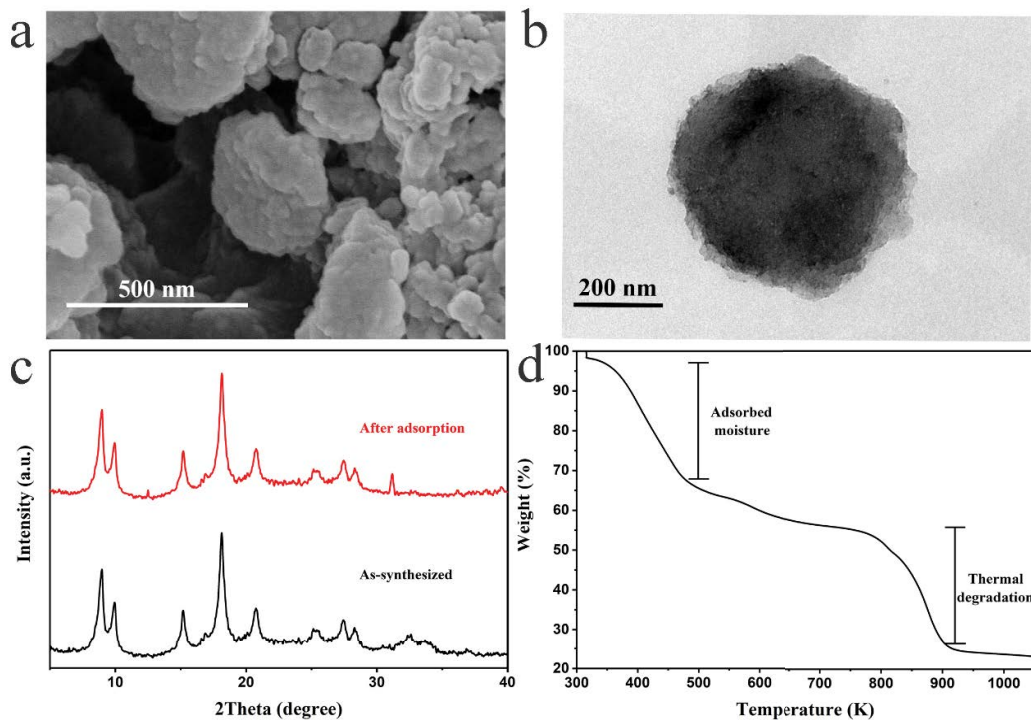


Fig. 1. SEM image of as-synthesized Al-MOF-5 (a), TEM image of as-synthesized Al-MOF-5 (b), XRD patterns of as-synthesized Al-MOF-5 before and after fluoride adsorption (c), and thermogravimetric analysis of Al-MOF-5 (d).

that the material consisted of stacked lamellar crystals; crystal stacking had left gaps in the surface and the stacking was uneven, which in turn resulted in a slight unevenness in size. Such a structure increases the specific surface area of a material. The TEM image (Fig. 1b) reveals a nanosheet cluster-like structure, with the thin nanosheet layer having an average size of about 200 nm.

The XRD pattern shown in Fig. 1c indicates that the material contained  $\text{Al}_2\text{O}_3$  crystals with good crystallinity. The most intense peak, appearing at  $2\theta = 18.062^\circ$ , corresponds to the carbon peak of organic matter. Since the experimentally prepared MOF was synthesized using 1,4-benzenedicarboxylic acid and  $\text{Al}(\text{NO}_3)_3 \cdot 9\text{H}_2\text{O}$ , the formed  $\text{Al}_2\text{O}_3$  was coated with an organic framework, which decreased the intensity of the  $\text{Al}_2\text{O}_3$  peak. The baseline drift and reduction in peak intensity are consistent with covering of the metal element; this is characteristic of MOFs. There was no significant change in the XRD pattern or the SEM morphology after adsorption, which indicated that the Al-MOF-5 was stable [25,26].

Fig. 1d shows the changes in chemical and physical properties of Al-MOF-5 as a function of temperature. The thermogravimetry (TG) curve indicates two weight loss processes between the starting temperature and 1,000 K. About 3% of the weight loss before 373 K is attributed to the evaporation of adsorbed surface water. This was not surprising because the final step of the synthesis involved low-temperature drying at 333 K. The second event near 426 K likely corresponds to the evaporation of residual DMF. The Al-MOF-5 began to degrade at about 800 K, which demonstrates that it can be safely used for adsorption purposes in water treatment.

The BET nitrogen adsorption isotherm and nascent pore size distribution are shown in Fig. 2. The isotherm was of type IV and increased steeply when  $P/P_0 < 0.05$ , and then equilibrated at higher pressures. The limiting value was obtained when  $P/P_0$  approached unity, at which point a very obvious rise occurred [27]. Adsorption hysteresis loops appeared in the middle section, which is indicative of capillary condensation in a porous adsorbent. At moderate relative pressures, the rise was faster due to this condensation. Once the capillary agglomeration filled the mesopores, if the adsorbent has large pores or strong interactions with the adsorbate molecules, a multimolecular layer continues to build, and the adsorption isotherm continues to rise. However, in most cases, an adsorption termination platform occurs at the end of capillary condensation and no multimolecular layer adsorption occurs. These characteristics of the isotherm are consistent with the prepared Al-MOF-5 being mesoporous. The specific surface area of the Al-MOF-5 was  $1,264 \text{ m}^2/\text{g}$ , which is higher than that of activated alumina. The average pore size was 3.12 nm, but the pore size distribution suggests that the structure contained mesopores with microporous characteristics.

### 3.2. Effect of adsorbent dosage

The effect of adsorbent dosage on fluoride removal rate is evident in Fig. 3. The removal rate increased sharply with increasing Al-MOF-5 dosage but the change in the removal rate and adsorption capacity then began to decrease, and

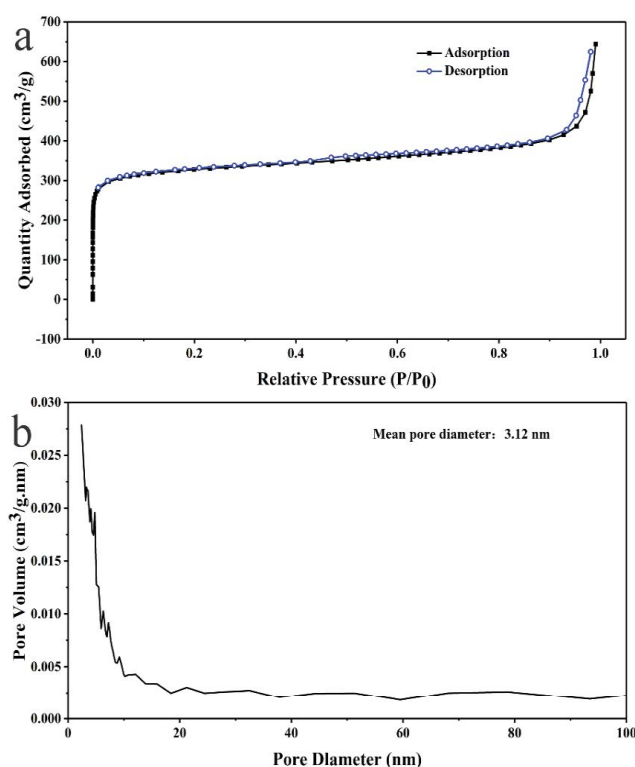


Fig. 2.  $\text{N}_2$  adsorption–desorption isotherms of as-synthesized Al-MOF-5 (a) and pore size distribution of Al-MOF-5 (b).

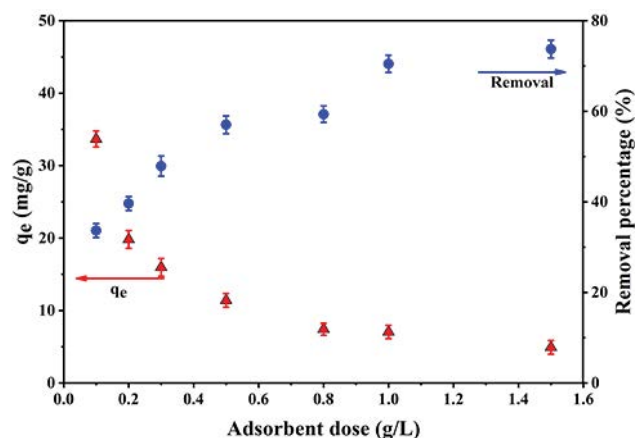


Fig. 3. Effect of adsorbent dosage on adsorption capacity and removal percentage of Al-MOF-5 (range of adsorbent dosage: 0.1–1.5 g/L; initial concentration of fluoride: 10 mg/L; volume of solution: 100 mL; pH: neutral; reaction time: 12 h; temperature: room temperature).

became negligible once the dosage reached 1.0 g/L. At relatively low adsorbent dosages, it was expected that the scarce adsorption sites would result in lower removal rates. However, although the number of adsorption sites was low, the fluoride concentration in the water was high, so utilization of the adsorption sites was high and the amount absorbed by the adsorbent was also high. With increasing dosage, the number of adsorption sites provided

by the adsorbent increased, yet the adsorption capacity decreased. This behavior was attributed to incomplete saturation of the active sites on the surface of the adsorbent during fluoride adsorption, which is consistent with a large number of active sites on the surface of the Al-MOF-5. We used the 1.0 g/L dosage level to evaluate the effect of pH and identify the optimal removal rate.

### 3.3. Effect of pH

It is well-known that the initial pH of a solution plays a very important role in the adsorption of a target contaminant by an adsorbent. We conducted experiments using solutions having an initial pH ranging from 3 to 11 to investigate the effect of pH on fluoride adsorption by Al-MOF-5.

Fig. 4 shows that the fluoride removal rate increased significantly under acidic and alkaline conditions, and the fluoride removal rate reached 100% in strong acids and bases. This behavior is mainly due to fluoride ions reacting with hydrogen ions under acidic conditions to form hydrofluoric acid, which is a weak electrolyte. Although fluoride is soluble in water, it is partially present in the form of molecules such that, in the presence of adsorbents, the removal rate will increase with decreasing pH. Under acidic conditions, hydrofluoric acid competes for adsorption, leading to a decrease in the fluoride ion concentration. We did not add adsorbent to the fluoride solution under acidic conditions. The concentration of fluoride in the water did decrease; the fluoride content was almost zero at pH 3. However, the hydroxide ions in the solution, together with the Al ions bridging the organic skeleton of the material, caused flocculation. This resulted in the removal of fluoride ions from the water. Thus, the removal rate also significantly increased under alkaline conditions [28]. The pH of the fluoride solution was adjusted to pH 9, 10, and 11 with NaOH, to study the effect of basicity on adsorption. After shaking for 12 h, the fluoride concentration of the solution had not changed significantly, although there may have been factors other than pH that affected the adsorption properties of the material. To exclude such pH-related complications,

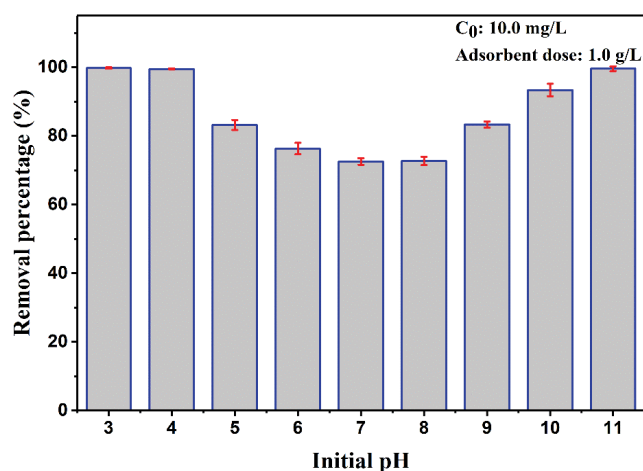


Fig. 4. Effect of pH on the removal percentage of Al-MOF-5 to fluoride (range of pH: 3–11; volume of solution: 100 mL; reaction time: 12 h; temperature: room temperature).

the following experiments were carried out under neutral conditions.

### 3.4. Fluoride adsorption isotherm

The interaction between analyte and adsorbent can be described by the adsorption isotherm. The Freundlich and Langmuir isotherm equations are widely used in adsorption isotherm models [29,30]. The D–R isotherm model is also often used to establish whether the adsorption mechanism is physical or chemical [31]. There is no theoretical model describing the adsorption isotherm for liquid adsorption. The adsorption isotherm model for gas adsorption is always used to describe liquid adsorption. Hence, we used these three models to describe the adsorption of Al-MOF-5 at different temperatures (Fig. 5). Visual inspection revealed that the isotherm was of the Langmuir type, and clearly endothermic. The adsorption amount of Al-MOF-5 gradually increased with increasing temperature and concentration.

The obtained results were fitted to the three isotherms using Eqs. (3)–(7) [29–31]:

Freundlich model:

$$\log q_e = \log K + \frac{1}{n} \log C_e \quad (3)$$

Langmuir model:

$$\frac{C_e}{q_e} = \frac{1}{q_0 b} + \frac{C_e}{q_0} \quad (4)$$

D–R model:

$$\log q_e = \ln q_0 - \beta \varepsilon^2 \quad (5)$$

$$\varepsilon = RT \ln \left( 1 + \frac{1}{C_e} \right) \quad (6)$$

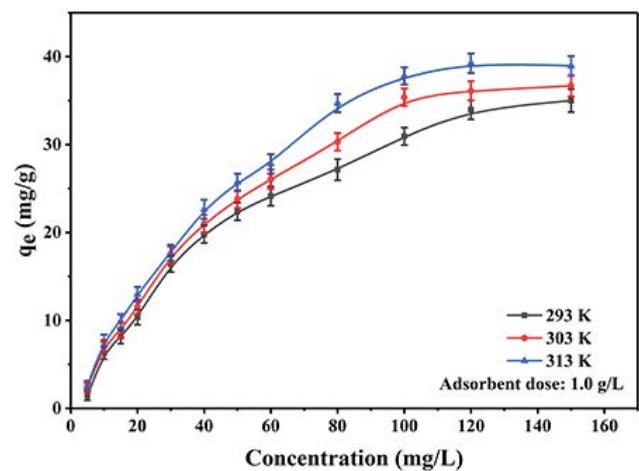


Fig. 5. Adsorption isotherms of fluoride under different reaction temperature (adsorbent dosage: 1.0 g/L; initial concentration of fluoride: 5–150 mg/L; pH: neutral; volume of solution: 100 mL; temperature: 293, 303, and 313 K; reaction time: 12 h).

$$E = \frac{1}{\sqrt{(2\beta)}} \quad (7)$$

where  $C_e$  (mg/L) is the concentration of fluoride remaining in the solution when adsorption equilibrium is reached,  $q_e$  (mg/g) is the adsorption amount at equilibrium,  $q_0$  (mg/g) is the single-layer adsorption amount at saturation, and  $K$ ,  $n$ , and  $b$  are constants. In the D–R model,  $\varepsilon$  (J/mol) is the Polanyi potential,  $k$  (mol<sup>2</sup> kJ<sup>-2</sup>) is a constant related to the adsorption energy,  $R$  is the universal gas constant, and  $E$  (kJ/mol) is the free energy of adsorption. For  $E = 8$ – $16$  kJ/mol, the adsorption process is triggered by ion exchange; for  $E < 8$  kJ/mol, physical forces such as van der Waals and hydrogen bonding may affect the adsorption mechanism; for  $E > 16$  kJ/mol, the adsorption process is of a chemical nature [31].

The important dimensionless constant  $R_L$  in the Langmuir model can be expressed as Eq. (8) [32]:

$$R_L = \frac{1}{1 + b \times C_0} \quad (8)$$

where  $b$  is the adsorption equilibrium constant and  $C_0$  is the initial concentration of the target pollutant. When  $0 < R_L < 1$ , adsorption occurs readily. When  $R_L = 0$ , adsorption is irreversible. When  $R_L = 1$ , the isotherm is linear and adsorption is reversible. When  $R_L > 1$ , adsorption is difficult [32].

Fig. 6 shows the theoretical Freundlich and Langmuir isotherms; the Langmuir isotherm showed better linearity. However, the data in Tables 1 and 2 pertaining to the removal of fluoride from Al-MOF-5 were better-fitted by the Langmuir model. At each temperature, the correlation coefficient  $R^2$  of the Langmuir model was significantly

higher than that of the Freundlich model. As the temperature increased,  $q_0$  and  $b$ , that is, the adsorption capacity and adsorption rate of Al-MOF-5, also increased. The calculated  $R_L$  value was also much less than unity at the various temperatures, which indicated that adsorption occurred readily. Although the Freundlich model had a low correlation coefficient, the value of  $1/n$  was about 0.5, suggesting that adsorption occurred. Furthermore, the value of  $1/n$  decreased with increasing temperature, which indicated that higher temperature assisted the adsorption process. The D–R isothermal model does not assume a uniform adsorbent surface or constant adsorption energy. The fitting results of the Freundlich and Langmuir models were used to establish whether physical or chemical adsorption occurred. The fitting results of the D–R adsorption model (Table 3) gave a free energy  $E = 8$ – $16$  kJ/mol. Although the data were poorly correlated, it is likely that the adsorption process was triggered by ion exchange. Fluoride adsorption by Al-MOF-5 was thus mainly single-layer adsorption triggered by ion exchange. Under neutral conditions at 313 K, the maximum adsorption capacity reached 46.08 mg/g.

### 3.5. Fluoride adsorption kinetics

Adsorption rate is another important index to characterize the adsorption capacity of adsorbents. The results of the kinetic study are shown in Fig. 7a. Although adsorption equilibrium was attained after 2 h, rapid adsorption took place within the first 30 min; only minor changes occurred during the last hour. This demonstrated that the large specific surface area of Al-MOF-5 provided good conditions for fluoride adsorption. The kinetics of this adsorption process were determined by fitting the data to pseudo-first-order, pseudo-second-order, and Elovich

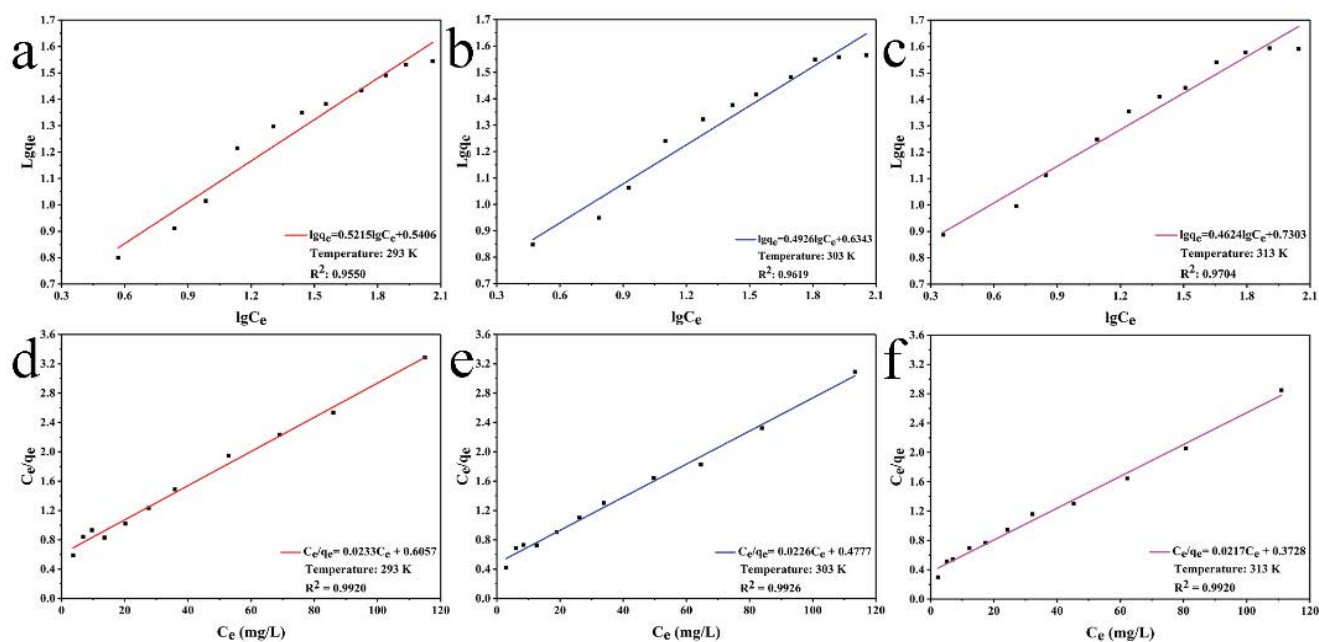


Fig. 6. Freundlich isotherm fitting at 293 K (a), 303 K (b), and 313 K (c) and the Langmuir isotherms isotherm fitting at 293 K (d), 303 K (e), and 313 K (f).

Table 1  
Fitted result by Freundlich model at different temperatures

Temperature (K)	Parameter			Linear equation
	$K$	$1/n$	$R^2$	
293	3.4722	0.5215	0.9550	$\log q_e = \log K + \frac{1}{n} \log C_e$
303	4.3082	0.4926	0.9619	$\log q_e = 0.4926 \log C_e + 0.6343$
313	5.3740	0.4624	0.9704	$\log q_e = 0.4624 \log C_e + 0.7303$

Table 2  
Fitted result by Langmuir model at different temperatures

Temperature (K)	Parameter			Linear equation
	$b$	$q_0$ (mg/g)	$R^2$	
293	0.0385	42.9185	0.9920	$C_e/q_e = 0.0233C_e + 0.6057$
303	0.0473	44.2478	0.9926	$C_e/q_e = 0.0226C_e + 0.4777$
313	0.0582	46.0829	0.9920	$C_e/q_e = 0.0217C_e + 0.3728$

Table 3  
Fitted result by D–R model at different temperatures

Temperature (K)	Parameter			Linear equation
	$E$ (kJ/mol)	$q_0$ (mg/g)	$R^2$	
293	12.3091	31.0469	0.8995	$\log q_e = -0.0033\varepsilon^2 + 3.4355$
303	14.1421	32.1625	0.8657	$\log q_e = -0.0025\varepsilon^2 + 3.4708$
313	12.5000	39.2794	0.9596	$\log q_e = -0.0032\varepsilon^2 + 3.6707$

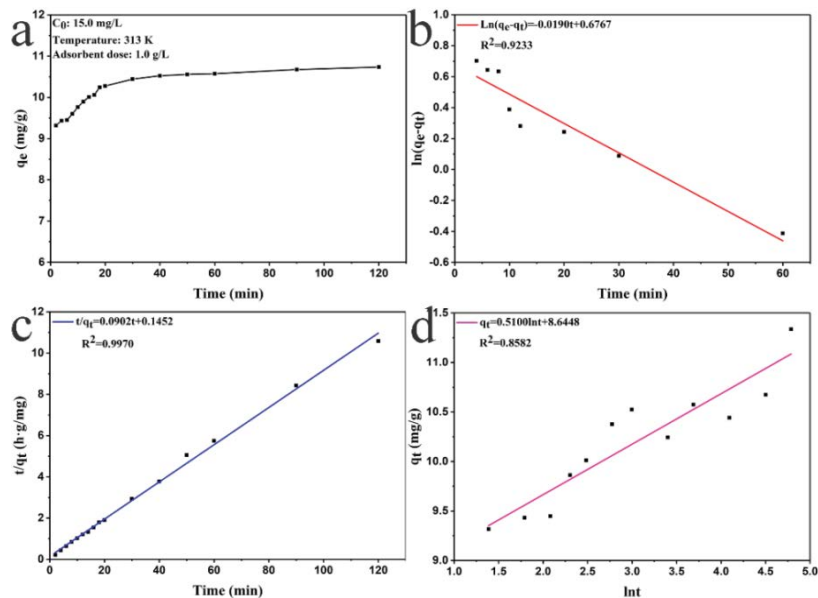


Fig. 7. Adsorption kinetic curve of fluoride by Al-MOF-5 (a), fit curve of pseudo-first-order model (b), fit curve of pseudo-second-order model (c), fit curve of Elovich model (d) (adsorbent dosage: 1.0 g/L; initial concentration of fluoride: 15 mg/L; pH: neutral; volume of solution: 100 mL; temperature: 313 K; reaction time: 2 h).

models (Eqs. (9)–(11) and Figs. 7b–d, respectively) [33,34]. The kinetic parameters are given in Table 4.

*Pseudo-first-order model:*

$$\ln(q_e - q_t) = \ln q_e - k_1 t \quad (9)$$

*Pseudo-second-order model:*

$$\frac{t}{q_t} = \frac{1}{k_2 q_e^2} + \frac{t}{q_e} \quad (10)$$

*Elovich model:*

$$q_t = \alpha + k_e \ln t \quad (11)$$

where  $q_t$  (mg/g) is the amount of fluoride adsorbed at time  $t$ ,  $q_e$  (mg/g) is the amount of adsorption at equilibrium,  $k_1$  ( $\text{min}^{-1}$ ) and  $k_2$  (g/mg min) is the rate constant, and  $k_2 q_e^2$  represents the initial adsorption rate. Both  $k_e$  and  $\alpha$  are Elovich constants.

The adsorption clearly followed pseudo-second-order kinetics; this was obvious from visual inspection of Figs. 7b–d, and was confirmed by the high  $R^2$  value of 0.9970. The Elovich model is an empirical formula that describes the adsorption behavior of contaminants on a heterogeneous solid surface [34]. The model does not make any mechanistic assumptions concerning adsorbate–adsorbent interactions. However, the  $R^2$  value of 0.8582 for the Elovich model was somewhat low. The good fit to pseudo-second-order kinetics confirmed that adsorption occurred through sharing or exchange of ions between the adsorbent and sorbate; this was also consistent with the analysis of the fitting to the D–R model.

### 3.6. Fluoride adsorption thermodynamics

The effect of temperature on the adsorption process is carried out at three different temperatures (293, 303, and 313 K), and the thermodynamic parameters (Gibbs free energy change:  $\Delta G^\circ$ , free entropy change:  $\Delta S^\circ$ , and free enthalpy change:  $\Delta H^\circ$ ) were calculated by the following formula: Eqs. (12)–(14) [35]:

$$\Delta G^\circ = \Delta H^\circ - T\Delta S^\circ \quad (12)$$

$$\Delta G^\circ = -RT \ln K_c \quad (13)$$

where  $K_c$  is the equilibrium constant at a certain temperature,  $R$  is the universal gas constant,  $K_c = q_e/C_e$  indicating the affinity of adsorption. So, the above formulas can be combined to get:

$$\ln \frac{q_e}{C_e} = -\frac{\Delta H^\circ}{RT} + \frac{\Delta S^\circ}{R} \quad (14)$$

The positive enthalpy change ( $\Delta H^\circ$ ) noted in Table 5 indicates that the process of adsorbing fluoride by Al-MOF-5 was endothermic. The negative  $\Delta G^\circ$  value indicates that the process was spontaneous. In the solid–liquid adsorption system, two processes exist simultaneously, that is, the solute is adsorbed by an adsorbent in solution, and the solvent is desorbed into solution. The former corresponds to entropy reduction (reduced degrees of freedom) and the latter to an increase in entropy. The entropy change ( $\Delta S^\circ$ ) during the reaction is the sum of the two processes. The positive  $\Delta S^\circ$  found for fluoride adsorption by Al-MOF-5 indicates that the adsorption reaction was entropy-driven. Additionally, according to the adsorption exchange theory, for solid–liquid exchange adsorption, the exchange of solute molecules from the liquid phase to the solid–liquid interface decreases free energy, resulting in a decrease in entropy. Therefore, the adsorption of fluoride onto the surface of Al-MOF-5 should also be a process of entropy reduction, yet the results indicate that  $\Delta S^\circ$  was greater than zero. Entropy was increased by the unavoidable release of substances during fluoride adsorption by Al-MOF-5. The two competing processes offset each other, so that the final entropy of the system was positive. The kinetic analyses described above suggested that fluoride adsorption by Al-MOF-5 was an ion exchange process. Summarizing, the fluoride adsorption by Al-MOF-5 was a spontaneous, entropy-driven endothermic process [36,37].

### 3.7. Experimental study on the effect of coexisting anion

Water bodies typically contain fluoride and other anions. These coexisting anions may compete with fluoride ions, negatively affecting the fluoride removal rate of the adsorbent and reducing its adsorption capacity. We selected commonly coexisting anions ( $\text{PO}_4^{3-}$ ,  $\text{SO}_4^{2-}$ ,  $\text{NO}_3^-$ ,  $\text{CO}_3^{2-}$ , and  $\text{Cl}^-$ ) for our experiments; their effects are shown in Fig. 8.

The effects of three sample concentrations (5, 10, and 20 mg/L) were compared with those of the control (no added anions). Fig. 8 reveals that the adsorption capacity

Table 4  
Fitted result of adsorption kinetic models at 313 K

Dynamic mode	Parameter	$R^2$	Kinetic equation
Pseudo-first-order equation	$k_1$ 0.019	$q_e$ (mg/g) 1.9670	0.9233 $\ln(q_e - q_t) = -0.0190t + 0.6767$
Pseudo-second-order equation	$k_2$ 0.056	$q_e$ (mg/g) 11.086	0.9970 $t/q_t = 0.0902t + 0.1452$
Elovich model	$k_e$ 0.510	$\alpha$ 8.645	0.8582 $q_t = 0.5100 \ln t + 8.6448$

Table 5

Thermodynamic parameters for the adsorption (adsorbent dosage: 1.0 g/L; initial concentration of fluoride: 5–150 mg/L; pH: neutral; volume of solution: 100 mL; temperature: 293, 303, and 313 K; and reaction time: 12 h)

Temperature (K)	Parameter		
	$\Delta H^\circ$ (kJ/mol)	$\Delta S^\circ$ (kJ/mol)	$\Delta G^\circ$ (kJ/mol)
293			-0.8782
303	21.3013	74.4278	-1.2503
313			-1.6225

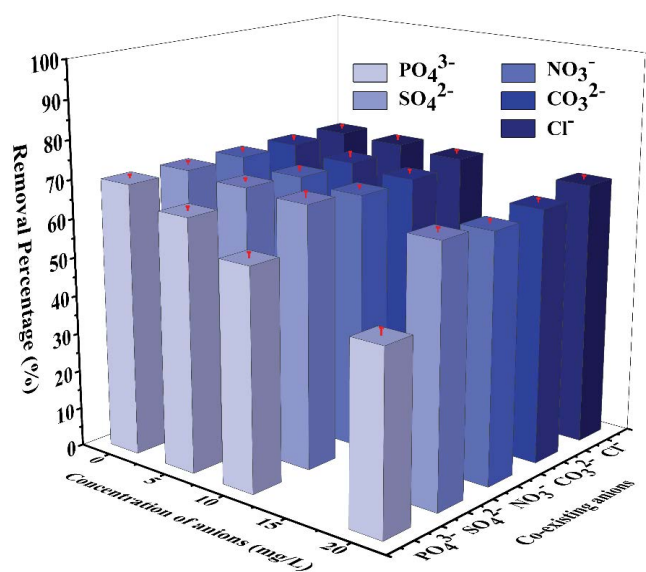


Fig. 8. Effect of co-existing anions on the removal percentage of Al-MOF-5 to fluoride (adsorbent dosage: 1.0 g/L; initial concentration of fluoride: 10 mg/L; pH: neutral; the volume of a solution: 100 mL; reaction time: 12 h; room temperature; co-existing anions:  $\text{PO}_4^{3-}$ ,  $\text{SO}_4^{2-}$ ,  $\text{NO}_3^-$ ,  $\text{CO}_3^{2-}$ , and  $\text{Cl}^-$ ).

of the adsorbent was affected by the coexisting anions to varying degrees. Phosphate ion had the greatest influence on the adsorption capacity, while the influence of the other four anions was almost negligible. A reduction in pH of the solution by anion addition should increase the removal rate; therefore, this can be ruled out as an explanation. It is more likely that the phosphate ion had a stronger affinity with the active sites on the surface of the adsorbent and competed with fluoride ions for these sites [38]. Notably, when the concentration of  $\text{PO}_4^{3-}$  ions was low, the removal rate remained close to 60%. This indicated that Al-MOF-5 has strong selective adsorption for fluoride and could be widely used to remove fluoride from water.

### 3.8. Fluoride adsorption mechanisms

Fig. 9 compares the FTIR spectra before and after fluoride adsorption by Al-MOF-5. The broad and strong absorption band at  $3441\text{ cm}^{-1}$ , and the peak at  $1641\text{ cm}^{-1}$ , are attributed to stretching vibrations of adsorbed water on

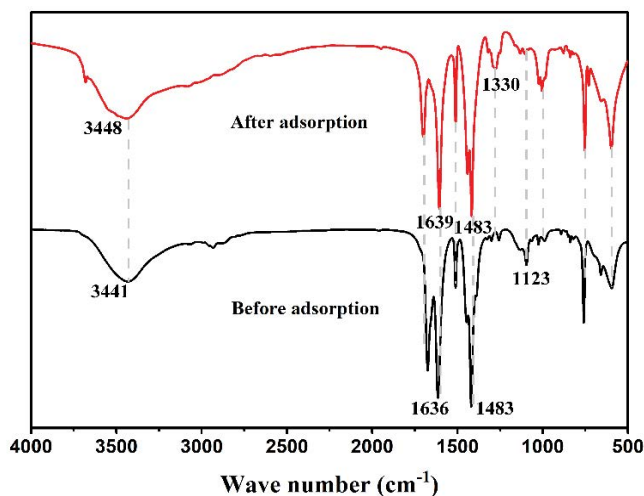


Fig. 9. FTIR spectra of Al-MOF-5 before and after adsorption.

Al-MOF-5 and bending vibrations of the hydroxyl group, respectively. Adsorption caused the peaks to shift to  $3448$  and  $1639\text{ cm}^{-1}$ , respectively, which suggested that  $\text{F}^-$  and  $\text{OH}^-$  underwent ion exchange on the Al-MOF-5 surface. The peak corresponding to the Al-OH moiety at  $1123\text{ cm}^{-1}$  disappeared after adsorption, with the appearance of a new peak at  $1330\text{ cm}^{-1}$ ; this was attributed to the formation of Al-F bonds and suggested that fluoride adsorption by Al-MOF-5 depended on the exchange of  $\text{OH}^-$  bound to Al within the material structure and to the strength of the interactions between interlayer anions and lattice cations [39,40]. The hydroxyl group was the active site that played a key role in the fluoride adsorption. In water,  $\text{F}^-$  replaced the  $\text{OH}^-$  groups on the adsorbent and combined with Al atoms to achieve defluorination. Ion exchange was central to fluoride removal by Al-MOF-5. After adsorption, the adsorbent could be regenerated by replacing  $\text{F}^-$  with  $\text{OH}^-$ , provided by a high concentration of NaOH solution.

XPS confirmed that fluoride adsorption by Al-MOF-5 occurred via an ion exchange process between  $\text{F}^-$  and  $\text{OH}^-$ . The F 1s peak at the binding energy of  $686.5\text{ eV}$  in the survey scan confirmed the adsorption of fluoride on the adsorbent (Fig. 10). High-resolution spectra of the Al 2p region showed that adsorption caused the binding energy to shift from  $74.38$  to  $74.28\text{ eV}$ . This indicated that a strong interaction had taken place between  $\text{Al}^{3+}$  and  $\text{F}^-$  ions during adsorption. Adsorption also caused a shift in the binding energy of the O 1s peak and a reduction in the peak area from  $53.4\%$  to  $43\%$ . This indicated that the  $\text{OH}^-$  groups on the surface of the sample participated in fluoride adsorption, and confirmed that the adsorption mechanism was ion exchange between  $\text{F}^-$  and  $\text{OH}^-$  [41,42].

### 3.9. Regeneration mechanisms

Adsorbent regeneration can greatly reduce the cost of removing pollutants from water. We established that ion exchange of  $\text{F}^-$  and  $\text{OH}^-$  was the adsorption mechanism governing fluoride adsorption by Al-MOF-5. Thus, NaOH solution was used as the regeneration solution. We also examined some other traditional regenerants, such as

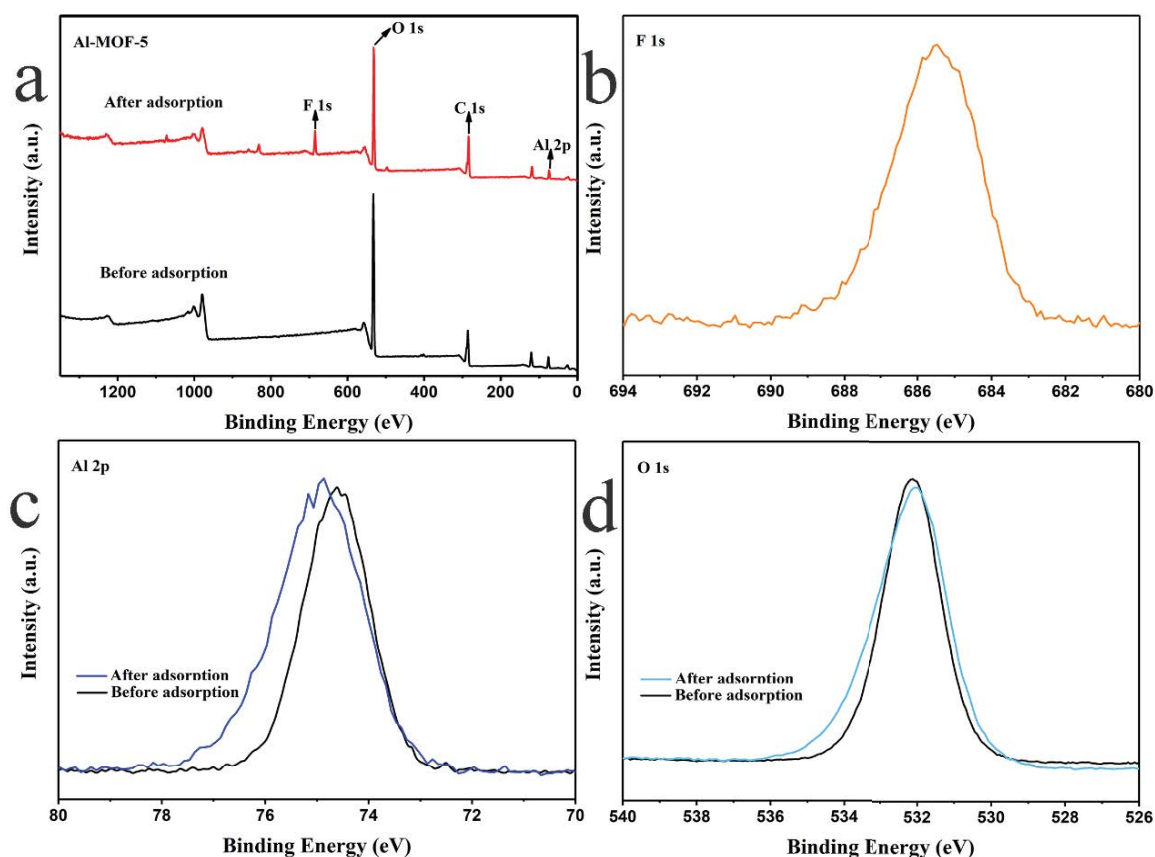


Fig. 10. XPS spectra of Al-MOF-5 before and after fluoride adsorption: XPS wide scan spectra of Al-MOF-5 before and after fluoride adsorption (a), XPS spectra of F 1s after fluoride adsorption (b), XPS spectra of Al 2p before and after fluoride adsorption (c), and XPS spectra of O 1s before and after fluoride adsorption (d).

hydrochloric acid and ethanol, but their regenerating abilities were unsatisfactory. Fig. 11 illustrates the recycling performance of NaOH-regenerated Al-MOF-5. As the concentration of the NaOH solution was increased over 24 h of regeneration, the fluoride removal rate initially increased and then decreased. The defluorination effect of Al-MOF-5 after regeneration was optimal at an NaOH concentration of 0.3 mol/L. The removal rate decreased at higher concentrations because some hydroxyl groups in solution adhered to the surface of the adsorbent, while others passed into the adsorbent, thereby destroying its structure. This resulted in lower fluoride removal after regeneration. Nevertheless, the material still displayed reasonable regenerative performance. At the optimal NaOH regenerant concentration, that is, 10 mg/L, a removal rate exceeding 50% was achieved after five recycling cycles. Finally, we compared the defluorination ability of Al-MOF-5 with some new and conventional adsorbents (Table 6). It is evident that Al-MOF-5 is an adsorbent with the strong defluorination ability and strong regenerative ability.

#### 4. Conclusion

We synthesized Al-MOF-5, a new MOF material, and used it to remove fluoride from water. This MOF had a specific surface area of 1,264 m<sup>2</sup>/g, and an adsorption

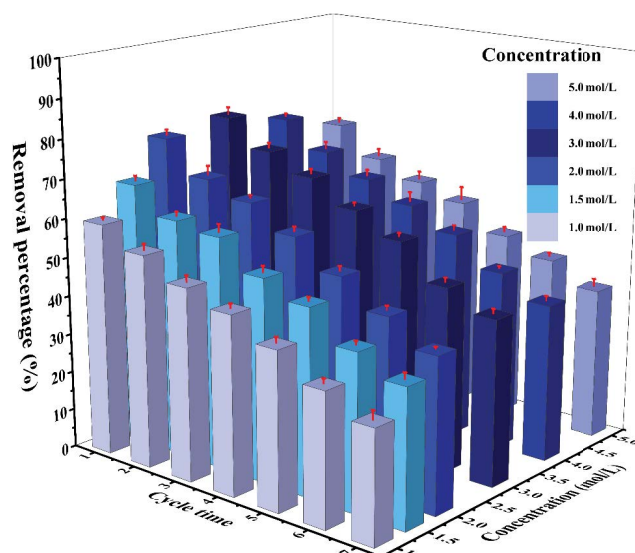


Fig. 11. Regeneration study of Al-MOF-5 using different concentrations of NaOH solution (adsorbent dosage: 1.0 g/L; initial concentration of fluoride: 15 mg/L; concentration of NaOH solution: 1.0, 1.5, and 2.0 mg/L; pH: neutral; volume of solution: 100 mL; temperature: room temperature; reaction time: 12 h).

Table 6  
Comparison of different adsorbents in literatures

Adsorbents	Adsorption capacity (mg/Fg)	Synthetic method	BET (m <sup>2</sup> /g)	Cycle times	Refs.
Activated alumina	14	N.R.	250	5	[43]
Ca–Al–La composite	29.3	Hydrothermal	N.R.	4	[44]
MgOC (magnesia/chitosan composite)	4.44	Calcination	45.5	N.R.	[45]
Mixed-rare earth magnetic chitosan beads	22.35	Inverse suspension	21.24	7	[46]
LDH (La-doped Li/Al layered double hydroxides)	34.8	Coprecipitation method	16	8	[24]
MIL(96)(Ce)	36.85	Hydrothermal	18.28	9	[47]
MOF-801	40	Hydrothermal	725	N.R.	[40]
This work	46.08	Hydrothermal	1,264	7	–

N.R.: non-reported.

capacity that reached 46.08 mg/g rapidly at 313 K. Thermodynamic study showed that the process of adsorption was spontaneous and endothermic, followed pseudo-second-order kinetics, and was consistent with the Langmuir adsorption isotherm model. Aluminum sites were the main active sites for fluoride adsorption. The results of FT-IR and XPS analyses, and of data fitting to the D–R model, established that the adsorption mechanism is ion exchange between the OH<sup>-</sup> of Al-MOF-5 and F<sup>-</sup>. Additionally, Al-MOF-5 displayed good fluoride removal performance at various pHs, even in the presence of SO<sub>4</sub><sup>2-</sup>, NO<sub>3</sub><sup>-</sup>, CO<sub>3</sub><sup>2-</sup>, and Cl<sup>-</sup>. It displayed excellent defluorination performance after several regeneration cycles. We conclude that Al-MOF-5 is a highly suitable adsorbent for fluoride removal from water. Therefore, this material is beneficial to the treatment of fluoride-containing wastewater in the industry. However, there are several challenges limit the usage of Al-MOF-5 at an industrial scale: (1) we need to find a cheaper synthesis method to reduce its production cost, so as to be widely used in practical industrial production. (2) The durability and adsorption capacity of the materials need to be further improved to ensure their reuse.

#### Data availability statement

The data used to support the findings of this study are included within the article.

#### Conflicts of interest

The authors declare that they have no conflicts of interest.

#### Acknowledgments

This study was funded by the National Natural Science Foundation of China (No. 51908252), the China Postdoctoral Science Foundation (No. 2019M652274), the Key Research and Development Project of Zhenjiang (No. 2016014, 2017022, and 2019022), the Qing Lan Project for Young Core Teachers in University of Jiangsu Province, and the Foundation from Marine Equipment and Technology Institute for Jiangsu University of Science and Technology, China (HZ20190004). We thank the anonymous reviewers for their constructive

comments that improved the manuscript. In addition, the English in this document has been checked by a company that provides professional English language editing services.

#### References

- [1] S. Karmakar, J. Dechnik, C. Janiak, S. De, Aluminium fumarate metal-organic framework: a super adsorbent for fluoride from water, *J. Hazard. Mater.*, 303 (2016) 10–20.
- [2] R.J. Carton, Review of the 2006 United States National Research Council report: Fluoride in drinking water, *Fluoride*, 39 (2006) 163–172.
- [3] S. Sobhanardakani, R. Zandipak, Cerium dioxide nanoparticles decorated on CuFe<sub>2</sub>O<sub>4</sub> nanofibers as an effective adsorbent for removal of estrogenic contaminants (bisphenol A and 17- $\alpha$  ethinylestradiol) from water, *Sep. Sci. Technol.*, 53 (2018) 1–13.
- [4] W.M. Edmunds, P.L. Smedley, Fluoride in Natural Waters, O. Selinus, Ed., *Essentials of Medical Geology*, Springer, Dordrecht, 2013, pp. 311–336.
- [5] H.G. Gorchev, G. Ozolins, WHO guidelines for drinking-water quality, *WHO Chron.*, 38 (1984) 104–108.
- [6] A. Rasool, A. Farooqi, T.F. Xiao, W. Ali, S. Noor, O. Abiola, S. Ali, W. Nasim, A review of global outlook on fluoride contamination in groundwater with prominence on the Pakistan current situation, *Environ. Geochem. Health*, 40 (2018) 1265–1281.
- [7] T.R. McClintock, Y. Chen, J. Bundschuh, J.T. Oliver, J. Navoni, V. Olmos, E.V. Lepori, H. Ahsan, F. Parvez, Arsenic exposure in Latin America: biomarkers, risk assessments and related health effects, *Sci. Total Environ.*, 429 (2012) 76–91.
- [8] M. Mohapatra, S. Anand, B.K. Mishra, E.G. Dion, P. Singh, Review of fluoride removal from drinking water, *J. Environ. Manage.*, 91 (2009) 67–77.
- [9] G. Viswanathan, S. Gopalakrishnan, S.S. Ilango, Assessment of water contribution on total fluoride intake of various age groups of people in fluoride endemic and non-endemic areas of Dindigul District, Tamil Nadu, South India, *Water Res.*, 44 (2010) 6186–6200.
- [10] E.J. Reardon, Y. Wang, A limestone reactor for fluoride removal from wastewaters, *Environ. Sci. Technol.*, 34 (2000) 3247–3253.
- [11] J. Singh, P. Singh, A. Singh, Fluoride ions vs. removal technologies: a study, *Arabian J. Chem.*, 9 (2016) 815–824.
- [12] S. Sobhanardakani, R. Zandipak, Synthesis and application of TiO<sub>2</sub>/SiO<sub>2</sub>/Fe<sub>3</sub>O<sub>4</sub> nanoparticles as novel adsorbent for removal of Cd(II), Hg(II) and Ni(II) ions from water samples: a state-of-the-art review, *Clean Technol. Environ.*, 19 (2017) 1913–1925.
- [13] S. Sobhanardakani, R. Zandipak, Removal of Janus Green dye from aqueous solutions using oxidized multi-walled carbon nanotubes, *Toxicol. Environ. Chem.*, 95 (2013) 909–918.
- [14] A. Rafique, M.A. Awan, A. Wasti, I.A. Qazi, M. Arshad, Removal of fluoride from drinking water using modified immobilized activated alumina, *J. Chem.*, 2013 (2013) 1–7.

- [15] A. Bhatnagar, E. Kumar, M. Sillanp, Fluoride removal from water by adsorption—a review, *Chem. Eng. J.*, 171 (2011) 811–840.
- [16] Y. Ku, H.M. Chiou, The adsorption of fluoride ion from aqueous solution by activated alumina, *Water Air Soil Pollut.*, 133 (2002) 349–349.
- [17] W.X. Gong, J.H. Qu, R.P. Liu, H.C. Lan, Adsorption of fluoride onto different types of aluminas, *Chem. Eng. J.*, 189 (2012) 126–133.
- [18] M.R. Azhar, P. Vijay, M.O. Tade, H. Sun, S. Wang, Submicron sized water-stable metal organic framework (bio-MOF-11) for catalytic degradation of pharmaceuticals and personal care products, *Chemosphere*, 196 (2018) 105–114.
- [19] X.X. Yue, W.L. Guo, X.H. Li, H.H. Zhou, R.Q. Wang, Core-shell  $\text{Fe}_3\text{O}_4/\text{MIL-101}(\text{Fe})$  composites as heterogeneous catalysts of persulfate activation for the removal of Acid Orange 7, *Environ. Sci. Pollut. Res.*, 23 (2016) 15218–15226.
- [20] H. Furukawa, K.E. Cordova, M. O’Keeffe, O.M. Yaghi, The chemistry and applications of metal-organic frameworks, *Science*, 341 (2013) 1230444, doi: 10.1126/science.1230444.
- [21] S.S. Kaye, A. Dailly, O.M. Yaghi, J.R. Long, Impact of preparation and handling on the hydrogen storage properties of  $\text{Zn}_4\text{O}$  (1,4-benzenedicarboxylate) (3) (MOF-5), *J. Am. Chem. Soc.*, 129 (2007) 14176–14177.
- [22] L.F. Harrington, E.M. Cooper, D. Vasudevan, Fluoride sorption and associated aluminum release in variable charge soils, *J. Colloid Interface Sci.*, 267 (2003) 302–313.
- [23] Z. He, R.P. Liu, J. Xu, H.J. Liu, J.H. Qu, Defluoridation by Al-based coagulation and adsorption: species transformation of aluminum and fluoride, *Sep. Purif. Technol.*, 148 (2015) 68–75.
- [24] J.G. Cai, X. Zhao, Y.Y. Zhang, Q.X. Zhang, B. Pan, Enhanced fluoride removal by La-doped Li/Al layered double hydroxides, *J. Colloid Interface Sci.*, 509 (2017) 353–359.
- [25] V.T. Van, H. Kosslick, A. Schulz, J. Harloff, E. Paetzold, H. Lund, U. Kragl, M. Schneider, G. Fulda, Influence of the textural properties of Rh/MOF-5 on the catalytic properties in the hydroformylation of olefins, *Microporous Mesoporous Mater.*, 154 (2012) 100–106.
- [26] D.P. Saha, Z.J. Wei, S.G. Deng, Hydrogen adsorption equilibrium and kinetics in metal-organic framework (MOF-5) synthesized with DEF approach, *Sep. Purif. Technol.*, 64 (2009) 280–287.
- [27] K. Michal, J. Mietek, Gas adsorption characterization of ordered organic-inorganic nanocomposite materials, *Chem. Mater.*, 13 (2011) 3169–3183.
- [28] L. Luo, K. Chen, Q. Liu, Y. Lu, T.A. Okamura, G.C. Lv, Y. Zhao, W.Y. Sun, Zinc(II) and cadmium(II) complexes with 1,3,5-benzenetricarboxylate and imidazole-containing ligands: structural variation via reaction temperature and solvent, *Cryst. Growth Des.*, 13 (2013) 2312–2321.
- [29] Y. Liu, Y.J. Liu, Biosorption isotherms, kinetics and thermodynamics, *Sep. Purif. Technol.*, 61 (2008) 229–242.
- [30] X. Zhu, Y.B. Tang, F.Y. Chen, S. Yu, X.G. Wang, Synthesis of magnetic rectorite/humic acid/chitosan composite for removal of heavy metal ions from water, *Desal. Water Treat.*, 163 (2019) 155–165.
- [31] R.A. Anayurt, A. Sari, M. Tuzen, Equilibrium, thermodynamic and kinetic studies on biosorption of Pb(II) and Cd(II) from aqueous solution by macrofungus (*Lactarius scrobiculatus*) biomass, *Chem. Eng. J.*, 151 (2009) 255–261.
- [32] E.K. Putra, R. Pranowo, J. Sunarso, N. Indraswati, S. Ismadji, Performance of activated carbon and bentonite for adsorption of amoxicillin from wastewater: mechanisms, isotherms and kinetics, *Water Res.*, 43 (2009) 2419–2430.
- [33] K.Y.A. Lin, Y.T. Liu, S.Y. Chen, Adsorption of fluoride to  $\text{UiO-66-NH}_2$  in water: stability, kinetic, isotherm and thermodynamic studies, *J. Colloid Interface Sci.*, 461 (2016) 79–87.
- [34] R.J. Atkinson, F.J. Hingston, A.M. Posner, J.P. Quirk, Elovich equation for the kinetics of isotopic exchange reactions at solid–liquid interfaces, *Nature*, 226 (1970) 148–149.
- [35] Q.S. Liu, T. Zheng, P. Wang, J.P. Jiang, N. Li, Adsorption isotherm, kinetic and mechanism studies of some substituted phenols on activated carbon fibers, *Chem. Eng. J.*, 157 (2009) 2–13.
- [36] W. Plazinski, W. Rudzinski, A. Plazinska, Theoretical models of sorption kinetics including a surface reaction mechanism: a review, *Adv. Colloid Interface Sci.*, 152 (2010) 348–356.
- [37] T. Madrakian, A. Afkhami, M. Ahmadi, H. Bagheri, Removal of some cationic dyes from aqueous solutions using magnetic-modified multi-walled carbon nanotubes, *J. Hazard. Mater.*, 196 (2011) 109–114.
- [38] Y. Li, P. Huang, D.D. Tao, J. Wu, M. Qiu, X. Huang, K.N. Ding, W.K. Chen, W.Y. Su, Y.F. Zhang, Adsorption and dissociation of  $\text{H}_2\text{S}$  on monometallic and monolayer bimetallic Ni/Pd (111) surfaces: a first-principles study, *Appl. Surf. Sci.*, 387 (2016) 301–307.
- [39] P. Kumar, A. Pournara, K.H. Kim, V. Bansal, S. Rapti, M.J. Manos, Metal-organic frameworks: challenges and opportunities for ion-exchange/sorption applications, *Prog. Mater. Sci.*, 86 (2017) 25–74.
- [40] X.G. Wang, H. Zhu, T.S. Sun, Y.B. Liu, T. Han, J.X. Lu, H.L. Dai, L.Z. Zhai, Synthesis and study of an efficient metal-organic framework adsorbent (MIL-96(Al)) for fluoride removal from water, *J. Nanomater.*, 3 (2019) 1–13.
- [41] L. Chen, K.S. Zhang, J.Y. He, W.H. Xu, X.J. Huang, J.H. Liu, Enhanced fluoride removal from water by sulfate-doped hydroxyapatite hierarchical hollow microspheres, *Chem. Eng. J.*, 285 (2018) 616–624.
- [42] H.B. Yao, Y. Li, A.T. Wee, An XPS investigation of the oxidation/corrosion of melt-spun Mg, *Appl. Surf. Sci.*, 158 (2000) 112–119.
- [43] S. Ghorai, K.K. Pant, Investigations on the column performance of fluoride adsorption by activated alumina in a fixed-bed, *Chem. Eng. J.*, 98 (2004) 165–173.
- [44] W. Xiang, G. Zhang, Y. Zhang, D. Tang, J. Wang, Synthesis and characterization of cotton-like Ca-Al-La composite as an adsorbent for fluoride removal, *Chem. Eng. J.*, 250 (2014) 423–430.
- [45] C.S. Sundaram, N. Viswanathan, S. Meenakshi, Defluoridation of water using magnesia/chitosan composite, *J. Hazard. Mater.*, 163 (2008) 618–624.
- [46] P. Liang, R.Q. An, R.F. Li, D.F. Wang, Comparison of  $\text{La}^{3+}$  and mixed rare earths-loaded magnetic chitosan beads for fluoride adsorption, *Int. J. Biol. Macromol.*, 111 (2018) 255–263.
- [47] X. Yang, S.S. Deng, F.M. Peng, T. Luo, A new adsorbent of a Ce ion-implanted metal-organic framework (MIL-96) with high-efficiency Ce utilization for removing fluoride from water, *Dalton Trans.*, 46 (2017) 1996–2006.